Accurate heat of formation for fully hydrided $LaNi_5$ via the all-electron full-potential linearized augmented plane wave approach

Yu-Jun Zhao[a)]
Department of Physics, South China University of Technology, Guangzhou 510640, People's Republic of China

A. J. Freeman
Department of Physics and Astronomy, Northwestern University, Evanston, Illinois 60208

(Received 9 May 2007; accepted 14 June 2007; published online 14 August 2007)

The heat of formation, ΔH_f, for $La_2Ni_{10}H_{14}$, an important property for hydrogen storage, was remarkably overestimated in calculations, and has discouraged the use of first principles total energy methods in the search for novel metal hydrides. Here, we employ the all-electron full-potential linearized augmented plane wave method within both the generalized gradient approximation (GGA) and the local density approximation (LDA), along with a unique treatment of the total energy of the H_2 molecule, which plays a critical role in ΔH_f determinations. The calculated electronic properties indicate that charge transfer from the interstitial region to the H atoms stabilizes $LaNi_5$ hydride. We find the calculated ΔH_f (−31.3 kJ/mol H_2) within GGA is in excellent agreement with experiment (∼−32 kJ/mol H_2), as are the predicted geometrical structures for $LaNi_5$ and $La_2Ni_{10}H_{14}$. Surprisingly, although LDA calculations underestimate the volume of $LaNi_5$ by 10.4%, the final value of ΔH_f (−31.2 kJ/mol H_2), is also in excellent agreement with experiment. © *2007 American Institute of Physics*. [DOI: 10.1063/1.2767200]

I. INTRODUCTION

The absence of a practical means for hydrogen storage has been a major difficulty in utilizing hydrogen as a fuel or energy carrier.[1] A solid hydrogen storage system, like metal hydrides, is reliable, simple to engineer, and much safer than the use of other phases, and so metal hydrides still attract the most attention because of their applications in a wide range of industrial fields; those associated with energy transfer and storage were proposed two decades ago, with the innovation of new heat management processes—hydride chemical heat pumps.[2] In particular, $LaNi_5$ and its alloys have attracted great interest due to their large hydrogen capacity, moderate stability and excellent electrochemical reactiveness. It is recognized that the heat of formation is the most fundamental and important quantity for hydrides—in particular, for application to hydrogen storage systems.[3]

Experimentally, $LaNi_5$ may store up to 6.4 atoms of hydrogen per unit cell, i.e., about 5.5×10^{22} H atom/cm^3, at a higher density than pure solid hydrogen (5.3×10^{22} H atom/cm^3).[4] The measured heat of formation, ΔH_f, at high hydrogen density for $LaNi_5$ is about −32 kJ/mol H_2.[4,5] However, recent theoretical calculations could not predict the correct heat of formation for $LaNi_5$ hydrides.[6,7] Tatsumi *et al.*[7] studied the heat of formation of $LaNi_5H_7$ with a plane-wave basis pseudopotential method; and obtained −45 kJ/mol H_2, which is approximately 50% more negative than experiment. This has discouraged the use of first principles total energy methods in the search for novel metal hydrides. Although the experiment value for heat of formation is obtained from the hydride with a slightly lower H concentration, it is believed that ΔH_f is not significantly changed from that of full hydride because ΔH_f is nearly independent of H concentration.[4] Very recently, Hector *et al.*[8] improved on these results by employing the well-known pseudopotential plane-wave method, and obtained −40 kJ/mol H_2 for ΔH_f, leaving about a 25% disagreement with experiment. Moreover, a ferromagnetic moment of 1.33 μ_B per $LaNi_5$ was found, whereas $LaNi_5$ is known to be paramagnetic,[9] which raised the specter of the possible failure of spin density functional theory.

To investigate these disagreements we turn to the all-electron full-potential linearized augmented plane wave (FLAPW) method,[10] which has earned its reputation on the accuracy of its total energy calculations. In the process, we focused on the fact that the total energy of the H_2 molecule plays a critical role in heat of formation calculations, as

$$\Delta H_f = \frac{1}{7}[E(La_2Ni_{10}H_{14}) - 2E(LaNi_5)] - E(H_2). \quad (1)$$

As is well-known, the total energies of $La_2Ni_{10}H_{14}$ and $LaNi_5$ can be obtained from the total energy calculations of their unit cells, but further approximations are required to determine the total energy of H_2 (e.g., supercell model, film model, etc.). The remarkable feature of Eq. (1) is that a 1% error in $E_{tot}(H_2)$ will produce more than a 100% error for ΔH_f, and so it is the critical quantity for precise theoretical predictions.

In this work, we employ our unique bulk/thin film FLAPW method to determine the structure and total energies for $LaNi_5$ and its full hydride—$La_2Ni_{10}H_{14}$, and in particular for the total energy of the H_2 molecule to calculate ΔH_f precisely. Indeed, we demonstrate that the calculated heat of formation and the geometry structure within generalized gra-

[a)]Electronic mail: zhaoyj@scut.edu.cn

dient approximation (GGA) are in excellent agreement with experiment, which again credits the high accuracy of the all-electron FLAPW method. Surprisingly, we also find a ferromagnetic moment of 1.38 μ_B for $LaNi_5$—which reveals this as an outstanding failure of spin density functional theory.

II. METHODOLOGY

Both the local density approximation (LDA)[11] and the GGA[12] are employed in the calculations. Core states (up to 5*s* for La and 2*p* for Ni) are treated relativistically, whereas while valence states are treated scalar relativistically. Muffin-tin (MT) sphere radii are chosen to be 2.80 and 1.80 a.u. for La and Ni, respectively. A MT radius of 0.65 a.u. is adopted for the calculation of the H_2 molecule in a film model due to the short H–H bond length, and 1.0 a.u. is used for calculations on $La_2Ni_{10}H_{14}$. To perform integrations in reciprocal space, we used a $4\times4\times4$ mesh for $LaNi_5$ and $4\times4\times2$ mesh for $La_2Ni_{10}H_{14}$ following the Monkhorst-Pack scheme[13]—or 192 effective **k** points in Brillouin zone (BZ) for $LaNi_5$ and 96 **k** points in the BZ for $La_2Ni_{10}H_{14}$, which keeps a nearly equivalent density in reciprocal space for both. When the **k** mesh is increased to $6\times6\times6$ for $LaNi_5$, the total energy changes within 0.5 mRy, which will only brings an error of 0.6% to ΔH_f. In the interstitial region for $LaNi_5$ and $La_2Ni_{10}H_{14}$ plane waves with energy cutoffs up to 29.2 Ry for the variational bases and 262.4 Ry for the charge and potential are employed. A key quantity, the convergence with respect to the energy cutoff (K_{max}) for plane waves, will be discussed later in detail. Within the MT spheres, lattice harmonics with angular momentum *l* up to 12 are adopted. For the hydrogen molecule, the film version of the FLAPW method is used with an energy cutoff for wave functions up to 56.3 Ry.

III. RESULTS AND DISCUSSIONS

A. Total energy of hydrogen molecule

As mentioned previously, as the theoretical total energy of the hydrogen molecule can be decisive for obtaining the correct heat of formation, a special treatment is applied to its calculation with the FLAPW film code. Here, in addition to the spherical and interstitial regions in the bulk code, one defines a vacuum region where the wave functions are products of two-dimensional (2D) plane waves and *z*-dependent functions which are solutions of the one-dimensional Schrödinger equation of the (x,y)-averaged potential in the vacuum region. This not only saves much computational effort, but allows higher precision for total energy calculations of film and molecules.[10]

The total energy is calculated in a 10 Å$\times$10 Å 2D unit cell within both LDA and GGA. Plane waves with an energy cutoff (K_{max}) up to 56.3 Ry are used as variational bases, whereas a 506.3 Ry energy cutoff (G_{max}) is used for the charge and potential; these high energy cutoffs severely limit errors to the total energy of H_2. The calculated total energies for H_2 are −2.288 and −2.333 Ry within LDA and GGA, respectively, and change only within 0.16 mRy (or ~1% of ΔH_f) when the unit cell size increases to 15 Å$\times$15 Å. Thus, we have the required precision in the calculated $E_{tot}(H_2)$.

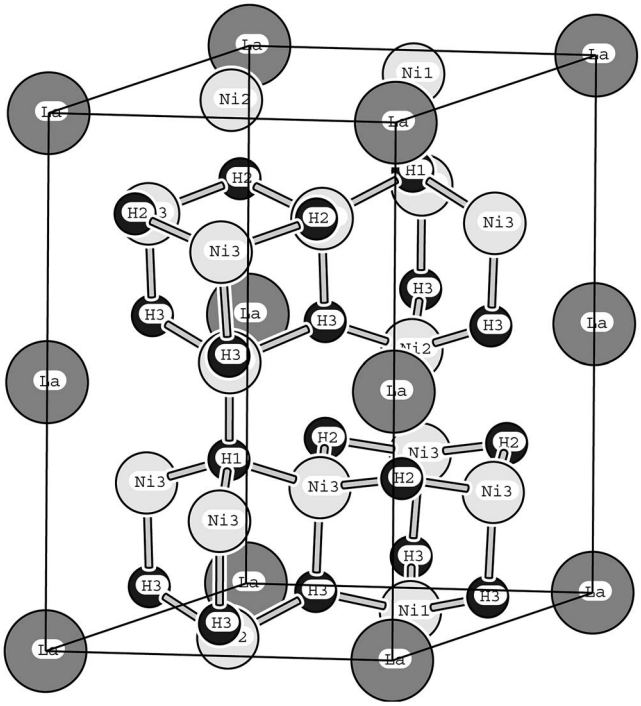

FIG. 1. The ball-stick model for the structure of $La_2Ni_{10}H_{14}$ labeled with the different atom types.

B. Heat of formation with experimental structure of $LaNi_5$ and $La_2Ni_{10}H_{14}$

At first, the experimental coordinates of $LaNi_5$ and $La_2Ni_{10}H_{14}$ were employed for the heat of formation calculations. $LaNi_5$ crystallizes in the $CaCu_5$-type structure with one formula unit per unit cell, space group of $P6/mmm$. The stablest hydride, $La_2Ni_{10}H_{14}$, has $P6_3mc$ symmetry with a doubled $LaNi_5$ unit cell along the *c* axis and hosts 14 hydrogen atoms. The structure of $La_2Ni_{10}H_{14}$ is shown in Fig. 1 with site type classifications for Ni and H. The experimental lattice parameters are $a=5.017$ Å, $c=3.970$ Å for $LaNi_5$ and $a=5.409$ Å, $c=8.600$ Å for $La_2Ni_{10}H_{14}$.[6]

Now, overcompleteness is a problem often encountered in total energy calculations with a high energy cutoff plane wave basis. In a usual diagonalization routine for general eigenvalue problems, the overlap matrix *S* is factorized by the Cholesky method assuming that the matrix *S* is positive definite. In some cases for an LAPW basis set, however, some eigenvalues of *S* could have almost zero value as there is a near linear dependence in the LAPW basis set, especially in the case of a very large energy cutoff for a plane wave basis, as in the total energy calculations in this work. For example, the total energy of $LaNi_5$ drops "anomalously" for K_{max} beyond 23 Ry which clearly shows the overcompleteness problem and causes trouble for ΔH_f calculations. Fortunately, the canonical orthogonalization method can circumvent this problem.[14] It diagonalizes the overlap matrix *S* and eliminates small eigenvalues less than a certain criterion (in

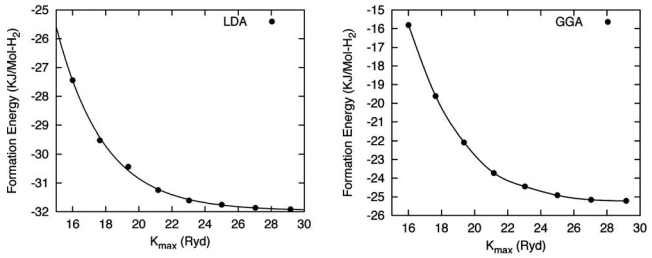

FIG. 2. The calculated heat of formation with respect to the increasing energy cutoff (K_{max}) for plane wave basis, within both the (left) LDA and (right) GGA. The experiment coordinates and lattice parameters are used for $La_2Ni_{10}H_{14}$ and $LaNi_5$. K mesh of $4\times4\times4$ for $LaNi_5$ and $4\times4\times2$ for $La_2Ni_{10}H_{14}$ are employed. The K_{max}'s for H_2 total energies are scaled according to $K_{max}\times R_{MT}$=constant.

our case, 10^{-6}) and their corresponding eigenvectors—namely, the (almost) linear dependent part of the LAPW basis functions.

Both $LaNi_5$ and $La_2Ni_{10}H_{14}$ were first treated nonspin polarized as they are known to be paramagnetic[9]; their magnetic properties will be discussed later. The convergence of the total energy of $LaNi_5$ and $La_2Ni_{10}H_{14}$ is rather slow—the total energy of $La_2Ni_{10}H_{14}$ stills goes down by more than 30 mRy when K_{max} increases from 25.0 to 29.2 Ry. Here, the convergence of ΔH_f is checked with respect to increasing K_{max}, which is shown in Fig. 2. Noticing that different R_{MT}'s are adopted for H in the H_2 and $La_2Ni_{10}H_{14}$ calculations, the total energy of H_2, $E_{H_2}(K_{max})$, is converted to $E_{H_2}(K_{max}/0.65)$ in order to keep $K_{max}\times R_{MT}$ the same in both, ΔH_f converges well as it changes by less than 10^{-1} kJ/mol H_2 when K_{max} increases from 25.0 to 29.2 Ry (see Fig. 2). It also shows that the GGA calculations converge slower than the LDA calculations due to the smaller localization of the exchange-correlation potential within GGA.

C. Structure optimization and formation energy

With the experimental lattice parameters and coordinates, the maximum residual force is more than 40 mRy/bohr within both LDA and GGA; thus, further relaxation is required for a more precise calculation of ΔH_f. Hence, the geometry structure of $LaNi_5$ and $La_2Ni_{10}H_{14}$ was fully optimized with a K_{max} of 19.4 Ry; the calculated forces show no remarkable changes when K_{max} increases to 25.0 Ry and higher. This indicates that the geometry structure converges much faster than the total energy with respect to the plane wave basis energy cutoff. The optimized lattice parameters for $LaNi_5$ and $La_2Ni_{10}H_{14}$ within both LDA and GGA are listed in Table I together with the total energies and the experimental lattice parameters. There are no changes in the internal structural parameters of $LaNi_5$ since its $P6/mmm$ structure is kept during the optimization.

The optimized $LaNi_5$ lattice within LDA shrinks along the $\langle1000\rangle$ and $\langle0100\rangle$ directions by 3.0% although it changes little along c in comparison with experiment. Obviously, the volume of the $LaNi_5$ unit cell is strongly underestimated (by 10.4%) within LDA. The volume of $La_2Ni_{10}H_{14}$ is also underestimated (by 4.4%) within LDA. The distance of H to the nearby Ni also shrinks in general. With the poor description of the $LaNi_5$ lattice volume, the LDA total energy of $LaNi_5$ is lower by 11.0 mRy compared with that of experiment lattice; this roughly cancels out the energy gain from relaxation for $La_2Ni_{10}H_{14}$. Surprisingly, and probably due to a cancellation of errors, the final optimized LDA results also give an excellent value for ΔH_f compared to experiment, −31.2 kJ/mol H_2.

On the other hand, the GGA results give very good lattice properties for both $LaNi_5$ and $La_2Ni_{10}H_{14}$ (c.f. Table I) that are in good agreement with a previous GGA result.[7] Details of the GGA optimized internal positions are listed in Table II, which are also close to experiment. For example, the distance of H atoms to nearby Ni atoms changes by less than 0.02 Å in comparison with experiment except that between H1 and Ni1 (enlarged by 0.05 Å). The total energy within GGA for optimized $LaNi_5$ and $La_2Ni_{10}H_{14}$ with K_{max} of 29.2 Ry are 1.6 and 38.9 mRy lower than those of the corresponding experimental structures, respectively. As a result, the formation energy for the fully relaxed structures is −31.3 kJ/mol H_2 at $T=0$ K. The thermal enthalpy contribution from H_2 is mostly canceled out from that of $LaNi_5$ and

TABLE II. The FLAPW optimized structural data for $La_2Ni_{10}H_{14}$ with the $P6_3mc$ symmetry within GGA.

Atom	Symmetry	x	y	z
La	C_{3v}	0	0	0.0259
Nil	C_{3v}	1/3	2/3	0.0082
Ni2	C_{3v}	1/3	2/3	0.4827
Ni3	C_{1h}	0.5003	0.4997	0.2514
HI	C_{3v}	1/3	2/3	0.8202
H2	C_{1h}	0.1561	0.8439	0.2849
H3	C_{1h}	0.5052	0.4948	0.0574

TABLE I. The FLAPW optimized lattice parameters, total energies for $LaNi_5$ and $La_2Ni_{10}H_{14}$, calculated with K_{max} of 29.2 Ry, and the finalized heat of formation within both the LDA and GGA obtained with the calculated $E_{tot}(H_2)$ values for H_2 (−2.288 Ry with LDA and −2.333 Ry with GGA).

	$LaNi_5$			$La_2Ni_{10}H_{14}$			
Parameters	a (Å)	c (Å)	E_{tot} (Ry)	a (Å)	c (Å)	E_{tot} (Ry)	ΔH_f (kJ/mol H_2)
LDA	4.866	3.796	−32 165.7998	5.301	8.470	−64 348.0522	−31.2
GGA	4.992	3.876	−32 203.8591	5.415	8.585	−64 424.2152	−31.3
Expt[a]	5.017	3.986	–	5.409	8.600	–	~−32.0[b]

[a]Reference 6.
[b]References 4 and 5.

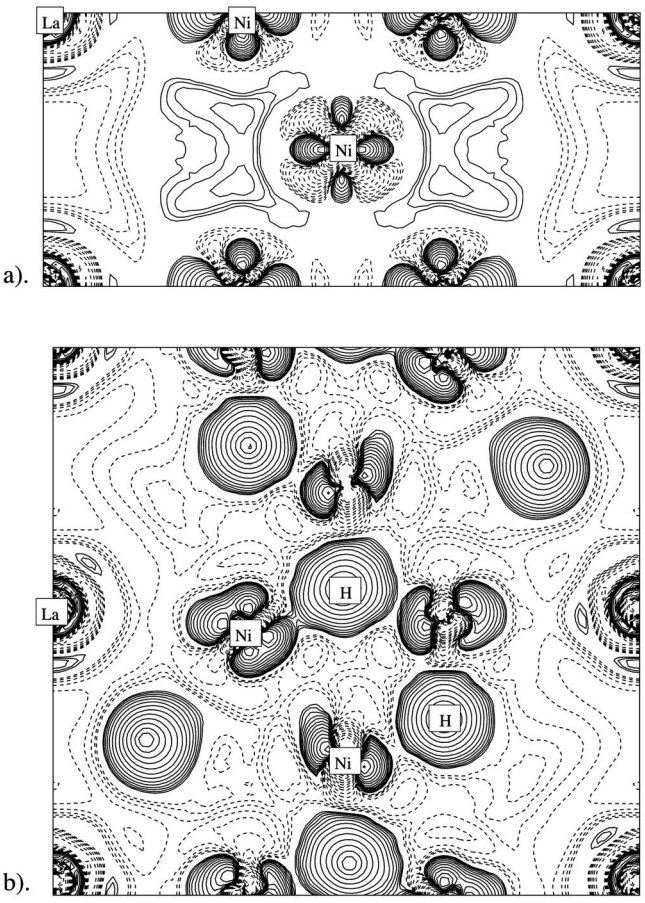

FIG. 3. The bonding charge density plot for optimized (a). $LaNi_5$ and (b). $La_2Ni_{10}H_{14}$ along $(2\bar{1}\bar{1}0)$ plane within GGA. Contours start from 10^{-3} e/a.u.^{3} and increase successively by a factor of $\sqrt{2}$. The solid and dashed lines denote the accumulation and depletion of charge density in comparison with the superstition of atomic density.

$La_2Ni_{10}H_{14}$, and it will not affect the heat of formation significantly.[7] Clearly, with the precise FLAPW calculation and the careful treatment of the total energy of H_2, the theoretical heat of formation is in excellent agreement with the experiment.[4,5]

In the next step, spin polarization is allowed in the $LaNi_5$ and $La_2Ni_{10}H_{14}$ systems; no further optimization is found due to little force change. In apparent contrast with experiment, $LaNi_5$ is found to be ferromagnetic with a magnetic moment of 1.38 μ_B per molecule unit within GGA, and 1.34 μ_B with LDA (converged at a k mesh of $8\times8\times8$). There is about 0.63 μ_B per molecule unit for $La_2Ni_{10}H_{14}$ at a k mesh of $4\times4\times2$, but it disappears as the mesh increases to $6\times6\times3$ (and denser) within both LDA and GGA. This is in good agreement with the work of Hector *et al.*,[8] although the magnetic properties converge more quickly on k points in our work. Further self-consistent calculations with spin–orbit coupling included changes the ferromagnetic state by only a small amount. Spin polarization lowers the total energy of $LaNi_5$ by about 2.9 mRy within GGA, and 1.8 mRy within LDA and changes the final heat of formation for $La_2Ni_{10}H_{14}$ to be −30.2 kJ/mol H_2 within GGA (−30.2 kJ/mol H_2 within LDA)—still in excellent agreement with experiment.

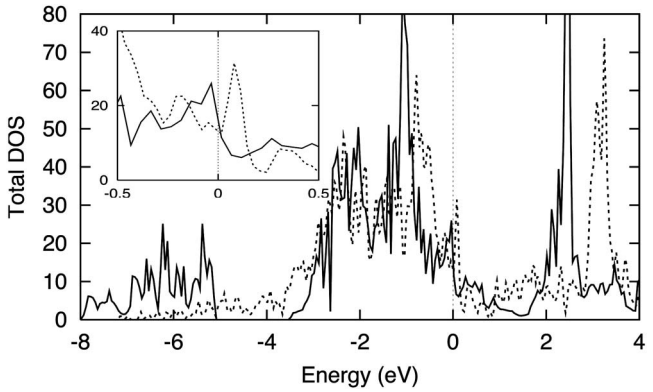

FIG. 4. The density of states for optimized $La_2Ni_{10}H_{14}$ (solid line) and $LaNi_5$ (dashed line—enlarged by a factor of 2 for a better comparison) within GGA. The inset panel shows the details of the DOS around E_F (taken as zero).

D. Electronic properties of $La_2Ni_{10}H_{14}$

Finally, we now consider the charge density, which plays the key role in an analysis of bonding mechanisms. As is well-known, the formation, dissolution, strengthening, and weakening of chemical bonds are always characterized by charge accumulation and depletion. The bonding charge density—the difference between the self-consistent density and the superposition of atomic densities with the same atomic geometry—is plotted in Fig. 3 for both $LaNi_5$ and $La_2Ni_{10}H_{14}$. It is clear that some electrons accumulate in the interstitial region around the center Ni atom in $LaNi_5$ [Fig. 3(a). After the full hydride is formed, most of the accumulated charges transfer to the H atoms, and lower the Coulomb energy.

The same physics is also seen from a comparison of the density of states (DOS) between $LaNi_5$ and $La_2Ni_{10}H_{14}$ in Fig. 4: the Ni $3d$ states are located ~3 eV below E_F, whereas the sharp peaks above E_F are from La $4f$, and the H $1s$ states are between ~8 eV and ~5 eV. Clearly, the sharp peak just above E_F in the $LaNi_5$ DOS (cf. the inset panel in Fig. 4) is shifted below E_F due to H solution, a result of states "dropping down" to the H $1s$ range from the Ni $3d$ region, and stabilizing the $LaNi_5$ full hydride.

In summary, the all-electron FLAPW first-principles total energy calculations give an excellent result on the heat of formation for $LaNi_5$ full hydride; the GGA results with fully relaxed structures give −31.3 kJ/mol H_2 (−30.2 if spin polarization is considered) for the heat of formation of $La_2Ni_{10}H_{14}$, in excellent agreement with experiment. This indicates that the all-electron FLAPW method is precise enough to aid in the design of hydrogen storage materials. It also gives an accurate description for the geometry structures of $LaNi_5$, and $La_2Ni_{10}H_{14}$. The bonding charge density of $LaNi_5$, and $La_2Ni_{10}H_{14}$ indicates that the H atom in $La_2Ni_{10}H_{14}$ attracts accumulated charges in the $LaNi_5$ interstitial region and lowers the total energy of $La_2Ni_{10}H_{14}$. The striking failure of spin density functional theory to properly treat the paramagnetic state of $LaNi_5$ calls attention to the need for new theoretical developments.

ACKNOWLEDGMENTS

Work supported by the NSF (through its MRSEC program at the Materials Research Center at Northwestern University) and a grant of computer time at the Arctic Region Supercomputing Center. The authors thank T. Shishidou and M. Yamaguchi for helpful discussions.

[1]Doped Carbon Nanotubes for Hydrogen Storage, Proceeding of the 2001 DOE Hydrogen Program Review, NREL, Golden, CO, 2001.
[2]P. Dantzer, *Hydrogen in Metals III, Topics in Applied Physics* (CRC Press, Boca Raton, FL, 1997), Vol. 73.
[3]K. Miwa and A. Fukumoto, Phys. Rev. B **65**, 155114 (2002).
[4]W. N. Hubbard, P. L. Rawlins, P. A. Connick, R. E. Stedwell, and P. A. G. O'hare, J. Chem. Thermodyn. **15**, 785 (1983).
[5]J. J. Murray, M. L. Post, and J. B. Taylor, J. Less-Common Met. **80**, 211 (1981).
[6]H. Nakamura, D. Nguyen-Manh, and D. G. Pettifor, J. Alloys Compd. **281**, 81 (1998).
[7]K. Tatsumi, I. Tanaka, H. Inui, K. Tanaka, M. Yamaguchi, and H. Adachi, Phys. Rev. B **64**, 184105 (2001).
[8]L. Hector, Jr., J. Herbst, and T. W. Capehart, J. Alloys Comp. **353**, 74 (2003).
[9]*Handbook on the Physics and Chemistry of Rare Earths*, edited by K. Gschneidner, Jr. and L. Eyring (North-Holland, Amsterdam, 1984), Vol. 6.
[10]E. Wimmer, H. Krakauer, M. Weinert, and A. J. Freeman, Phys. Rev. B **24**, 864 (1981).
[11]L. Hedin and B. I. Lundqvist, J. Phys. C **4**, 2064 (1971).
[12]J. P. Perdew, K. Burke, and M. Ernzerhof, Phys. Rev. Lett. **77**, 3865 (1996).
[13]H. J. Monkhorst and J. D. Pack, Phys. Rev. B **13**, 5188 (1976).
[14]A. Szabó and N. Ostlund, *Modern Quantum Chemistry: Introduction to Advanced Electronic Structure Theory* (Macmillan, New York, 1982).